ISSN 0015—3206
FZKAAA 23 (4) 333 (1991)

LASER-INDUCED FRACTAL CRACKING OF TUNGSTEN SURFACE

STJEPAN LUGOMER

Ruder Bošković Institute, POB 1016, 41001 Zagreb, Croatia

and

MLADEN STIPANČIĆ

Electrotechnical Faculty, University of Banja Luka, 78000 Banja Luka, Yugoslavia

Received 10 October 1991

UDC 538.951

Original scientific paper

Catastrophic response of tungsten surface in the Q-switched Nd:YAG laser-material interaction, on the average power density scale between $\overline{Q} = 1.4$ GW/cm^2 and $\overline{Q} = 3.5$ GW/cm^2 appears in the two typical crack morphologies: the line brittle crack and the ductile triangular crack. Both of them are treated as the fractal objects. For the first one, the fractal dimension $D = 1.60$ was found, and the comparison with the model of mechanical breakdown of elastic materials by Louis et al., and with the deterministic model of Takayasu is given. For the second one, the cavitation mechanism of growth on the triple junction is suggested. Its fractal modeling is based on the Apollonian gasket model with the characteristic fractal dimension $D \approx 1.32$. The crack velocity and the crack size have been estimated on the basis of the fracture mechanics model.

1. Introduction

Common characteristic of laser-material interactions on the power density scale of $Q = 10^9$ W/cm^2 and on the time scale of $\tau = 10^{-9}$ s is the plasma generation and the explosive expansion of the plasma ball, which generates the laser supported detonation wave (LSD)[1-6]. The LSD wave strikes the metal surface behind the expanding plasma, loading a pressure shock up to 10^8 Pa. The catastro-

phic response of the metal surface is the result of the pressure shock. However, at a lower power scale the plasma ball generated by the leading edge of the laser pulse becomes highly absorptive, and the rest of the laser pulse energy is deposited partially in the plasma and partially in the metal surface. Laser energy absorbed in the plasma is then reradiated on various wavelengths, in the second half of the laser pulse illuminating the metal surface, and increasing its temperature. In that case, catastrophic response of the surface is the result of both, the pressure shock and the temperature shock.

In the pulsed laser treatment at high repetition rate the process described above repeats many times in a second representing the cyclic pressure and temperature loading of the metal surface.

Catastrophic response of material surface on the laser energy deposition is spanning the range from the plastic deformation, cracking, to the crater formation (Refs. 7a, 7b). Every type of the surface response is of the threshold nature, and therefore it is determined (governed) by the characteristic average power density $\overline{Q}$, and by the material properties.

By the variation of the $\overline{Q}$-scale one is able to study variations in the type of catastrophic response of the material surface.

We have performed a series of experiments on refractory metals in order to study these effects: W, Ta and Mo, on the same set of $\overline{Q}$-scale values, and the great differences in their catastrophic response have been observed[7c]. In this letter we have concentrated on the catastrophic response of the tungsten surface, in particular on the cracking type of the surface response. The change of the $\overline{Q}$-scale switches the interaction from the laser-metal to the laser-plasma + laser-metal one. Since the increased temperature (in the second case) causes the increased plasticity, the surface response mechanism switches from the brittle cracking to the ductile one. The crack morphology changes also which was the reason that we payed attention on the geometrical and topological aspects of these cracks. The two basic configurations (corresponding to the two above mentioned cases) which may be treated as the fractal objects have been observed; a) the line crack, and b) the triangular crack.

2. *Experimental*

Mechanically polished plates of tungsten of ≈ 1.5 mm thickness were exposed to the pulsed treatment of a Q-switched Nd:YAG laser ($\lambda = 1.06$ μm) KORAD-44, with the following characteristics:

— laser peak power/pulse: 5 KW
— power density (adjustable up to): 10^9 W/cm^2
— energy density (adjustable up to): 100 J/cm^2
— pulse width: ≈ 200 ns.

Special KORAD optical head for work with metals and ceramics, with 4.4 cm focal distance was used.

The focal beam size was 90 μm in all cases.

The scan speed was constant 5 mm/s in all cases, while the pulse repetition frequency was varied from 6 kHz to 15 kHz. Since the system is equipped with the DEC PDP11 minicomputer, the experimental parameters have been varied by the variation of the input parameters.

The average power deposited $\overline{p}$ is given by:

$$\overline{P}(\mathrm{kW}) = \nu(\mathrm{Hz}) \times P_0(\mathrm{kW}) \tag{1}$$

where P_0 is the pulse peak power (5 kW), and ν is the pulse repetition frequency.

Variation of ν means the variation of $\overline{P}$. Since the irradiated surface in the unit of time was constant (scan velocity, $v = \mathrm{const}$), the change of the average power, means also the change of the average power density ($\overline{Q} = \frac{\overline{P}}{S}$, S=surface irradiated at a given scan velocity). Thus, we actually changed the $\overline{Q}$-scale in our experiments, from $\overline{Q} = 3.5\ \mathrm{GW/cm^2}$ to $\overline{Q} = 1.4\ \mathrm{GW/cm^2}$. The morphology of the surface response was studied by the SEM Leitz 2000 electron microscope.

3. *Results and discussion*

3.1. *Percolation of the broken bounds and broken bonds clustering*

The catastrophic response pattern of the tungsten surface on the laser energy deposition on the scale of $\overline{Q} = 3.5\ \mathrm{GW/cm^2}$, can be seen at different space scales in Figs. 1a and 1b. The cracks have characteristic of the transgranular (fast) cracking without presence of the »cusps«, »ledges«, »triple junctions«, or »twin boundary«, characteristics of the intergranular cracking.

Decreasing of the power density scale, to the $\overline{Q} = 2.4\ \mathrm{GW/cm^2}$ does not change the nature of the catastrophic response, as seen in Figs. 2a and 2b. On both power density scales, and on both space scales, the crack morphology does not change. In addition, $\approx 40\%$ of the cracks are transversely oriented to the laser scan direction. Here, we shall cut-off the scale size, becuse of two reasons: the first is, that the cracks on the size scale smaller than 0.1 μm (100 nm) are very difficult to observe, and the second is that the cracks on this scale are not stable. Their reversibility enable them to vanish, causing the result of observation to be taken with reserve.

Therefore, we limited our observation and analysis on the scales, on which the results of observation are reliable.

The mechanism of the crack growth is based on the percolation of the broken bonds and their coalescence.

During brittle cracking of tungsten, the individual bond breaking appear independently of its neighbours or position on the surface. Thus, the broken sites (bonds) percolate on the surface, their number increases with time and they finally coalesce into a crack, as seen in the micrography. The crack morphology is typical for transgranular brittle cracking. The cracks are self-similar which enables one to treat them as the fractal objects.

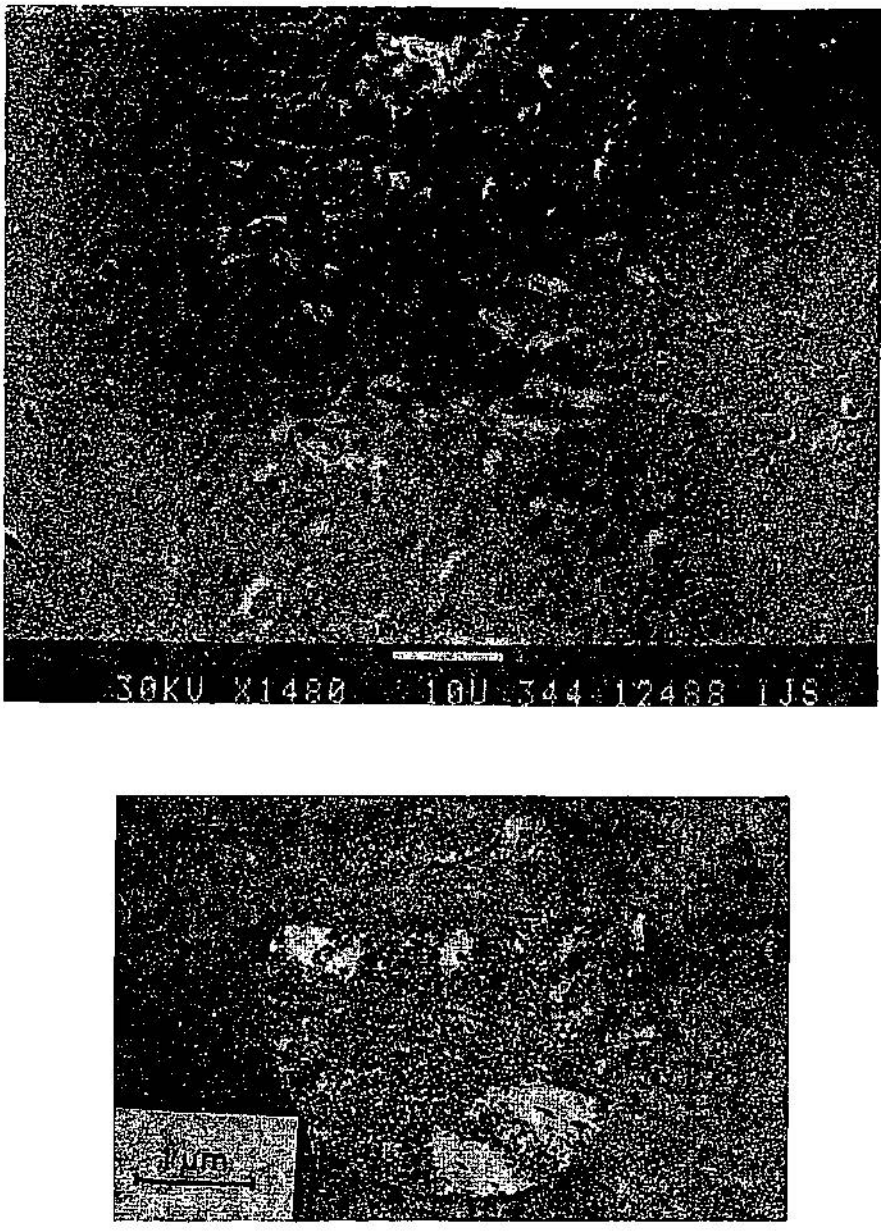

Fig. 1. The cracking pattern of tungsten surface as seen in the SEM micrography ($\nu = 15$ Hz, $v = 5$ mm/s, $\overline{Q} = 3.4$ GW/cm^2)

a) the space scale: 10 μm (10^4 nm)
b) the space scale: 1 μm (10^3 nm)

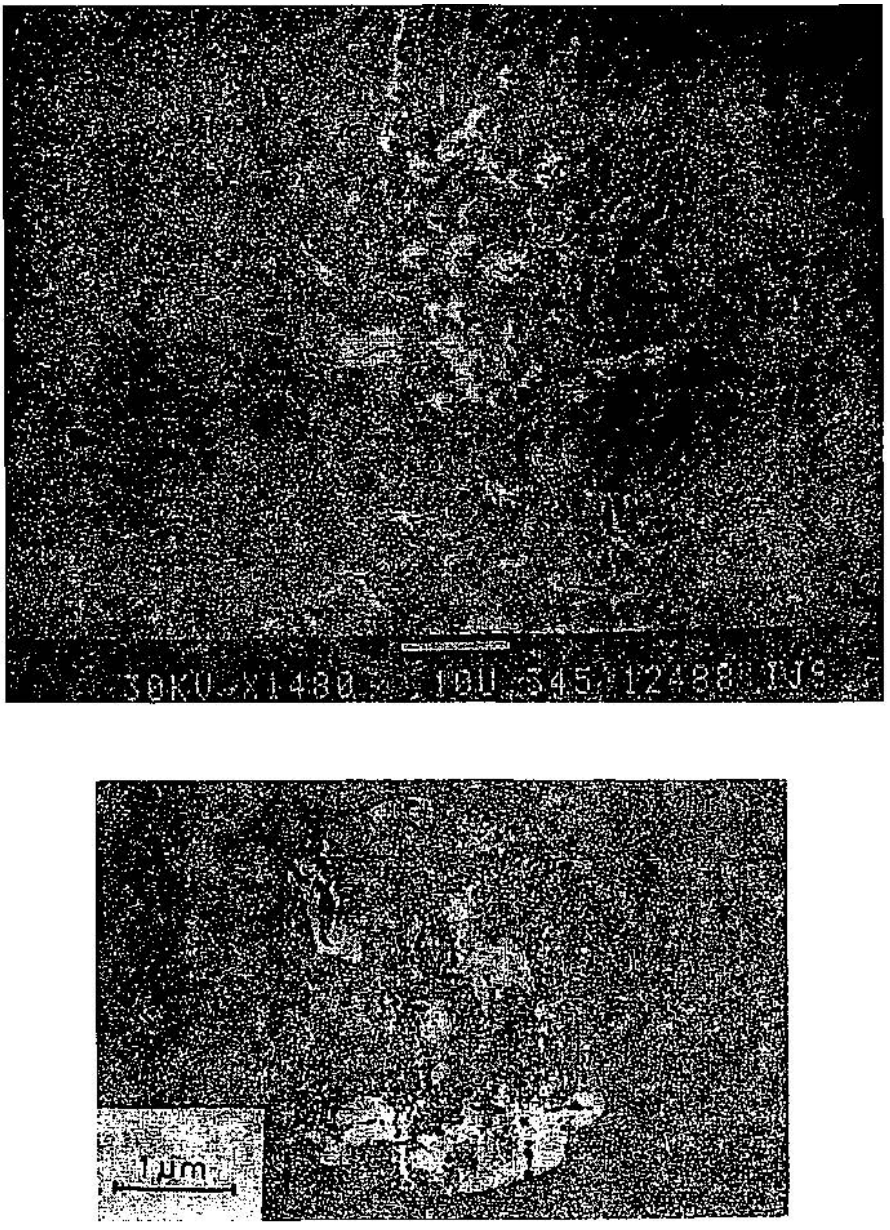

Fig. 2. The cracking pattern of tungsten surface as seen in SEM micrography (ν = 10 kHz, v = 5 mm/s, $\overline{Q}$ = 2.6 GW/cm^2)
a) the space scale: 10 μm (10^4 nm)
b) the space scale: 1 μm (10^3 nm).

The number of the broken bonds, N, is supposed to follow the power law:

$$N(r) \approx (r^2)^{\alpha}, \tag{2}$$

where α is the scalling exponent, which may be determined from the graphical presentation of the experimental results.

The number of the broken bonds, N, was determined by the standard procedure of the box counting:

— The frames, r^2 (nm^2), have been formed,

— The sum of the length of all the cracks in the given area (r^2), was found

— The sum was divided by the bond length.

By plotting the $N(r)$ vs area scale as given in Fig. 3 one is able to estimate the α value, which was found to be $\alpha = 0.79$. Using the Mandelbrot's area-length relation[8] (area)$^{1/2} \approx$ (length)$^{1/D}$ one finds the fractal dimensionality $D = 2\alpha$, which in our case gives: $D \approx 1.596$, or $D \approx 1.60$.

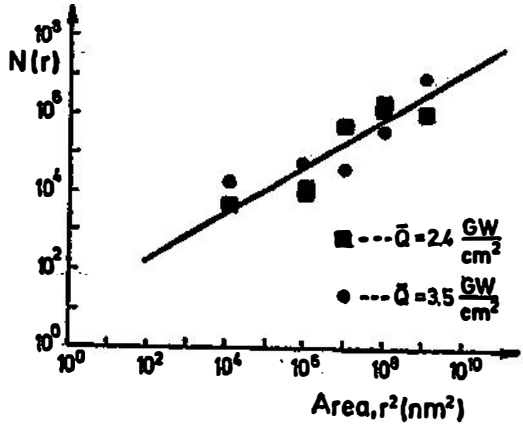

Fig. 3. The number of the broken bonds vs area for the two power scales $\bar{Q}$.

We shall compare this experimentally obtained value with the value obtained by the calculation from the appropriate theoretical models.

Some of the models of the fractal cracking of metals give the fractal dimension very different from $D = 1.60$. For example, the model of Lung[9] gives $D = 1.26$ which is to low, while the model of Meakin et al.[10] gives $D = 1.70$, which is to high value.

It seems that dimension $D = 1.60$ is in agreement with the dimension obtained by Louis et al.[11,12] from the model of mechanical breakdown for purely elastic materials, and with the dimension obtained by Takayasu from the deterministic model[13,14].

The model of Louis et al.[11,12] is vectorial counterpat of the scalar density field in DLA of Witen and Sander[15]. It is based on 2D triangular lattice of springs which simulates, in the continuum limit, an isotropic material. The chosen boundary conditions are unifrom expansion and shear deformation. The model starts with the lattice whose bonds are stretched by 10% over their equilibrium length. Then, a bond is broken and the lattice is allowed to relax to the new equilibrium state. The patterns obtained by simulation for 1200 broken bonds, consist of ramified clusters with the fractal dimension $D = 1.62 \pm 0.05$ and $D = 1.64 \pm 0.05$ for uniform expansion and shear, respectively[11]. In the other paper, Louis et al.[12] using the same model and 1500 broken bonds obtained $D = 1.55 \pm 0.05$ for uniform dilation and $D = 1.60 \pm 0.05$ for shear.

On this basis one could say that the model of Louis et al. very nicely describes the fractal nature of the laser induced cracks. However, the crack morphology, as seen from the micrographics, is not ramified (better, it is very poorly ramified). In addition, certain percentage of cracks are parallel between themselves, and finally, they are transversely oriented to the laser trace, or to the laser scan direction. These characteristics remind on the crack characteristics obtained on the basis of the Takayasu model[13,14]. This model is composed of brittle sticks; one end of a thin brittle stick of length unity is fixed while the other end is free. Displacement, d, larger than critical, d_c, causes that the stick gets broken. In this case, modulus of rigidity of the stick, G, which is defined by the ratio of the forceover the displacement may be approximately a constant until $d < d_c$, and when $d > d_c$, G may suddently be reduced to εG. where $(0 \leq \varepsilon \leq 1)$. The parameter ε denotes the ratio of reduction of rigidity and in the case of perfect fracture, $\varepsilon = 0$. When the stick has fractured then d becomes smaller than d_c, the modulus of rigidity keeps the reduced value εG. Thus, the process of fracture is modelled by the nonlinear inversible characteristics of modulus of rigidity. (The modulus of rigidity responds non-linearly to displacements).

The process is modelled on a plane square net consisting of brittle sticks that are connected stiffly at each lattice point. Displacements are perpendicular to the plane, which means that they result from the pure compressive stress in laser-material interaction.

The bond breakdown appears as the chain reaction initiated by the first bond breakdown spreading in its neighbourhood, and continues until the broken bonds form a percolation cluster.

Branches of the percolation crack, as well as the crack themselves, will be oriented from the first broken bond towards the end of the net, which gives the crack oriented transversaly to the laser scan direction. (The square net is supposed to be oriented with respect to the laser trace: one axis is parallel and another is transversal to the laser scan direction. The cracking process follows the shortest way to the net's end). Takayasu has found that the fractal dimensions is[13,14]:

$$D = 1.65 \pm 0.05 \tag{3}$$

which is in agreement to the limit of error with the value $D \approx 1.60$, found from the experiment.

It should be mentioned that the system is completely deterministic, that is, the growth procedure determines the evolution of the system uniquely for a given initial value $\{G\}$ and boundary condition of $\{\mu\}$.

Randomness of the crack patterns originates only from the randomness of the initial value of $\{G\}$[13,14].

Therefore we are inclined to the conclusion that the Takayasu model is a very probable one in this case, although the model of Louis et al.[11,12] gives a somewhat better agreement in the fractal dimensionality.

The above dilemma, whether the process is to be treated on the basis of the stochastic or deterministic model, is a very important one. If the cracking process is faster than any fluctuation (including thermal), than we have the so called quenched cracking, which is normally treated by the deterministic models[14]. However, if the cracking process is comparable with (thermal) fluctuations, than we have annealed cracking, which is normally treated by the stochastic models[14].

In the repetitive laser pulsing, the pulses are very short (ns time scale), and the question is, whether the cracking occurs only during pulses, or it continues in time between the pulses. The answer seems to depend on the repetition frequency: at the high repetition frequency the process is fast; at the reduced frequency, the process extends in time between the pulses (quasi-continuous cracking).

In general, the cracking process induced by laser is a very specific one and probably falls somewhere in between the annealed and the quenched processes[14]. This may explain the fact that the experimental results may be compared to the results of the stochastic and deterministic models.

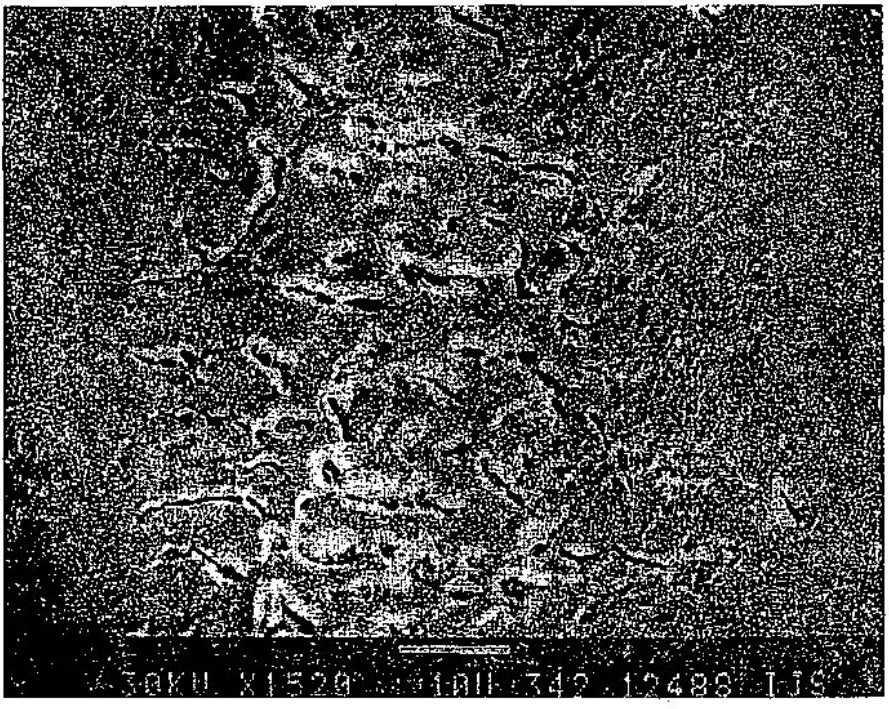

Fig. 4. The cracking pattern of tungsten surface as seen in SEM micrography ($\nu = 6\,\mathrm{kHz}$, $v = 5\,\mathrm{mm/s}$, $\overline{Q} = 1.4\,\mathrm{GW/cm^2}$).

3.2. *Percolation of vacancies and vacancy clustering into cavities: Cavity coalescence*

Decreasing the power density scale up to $\overline{Q} = 1.4\ \mathrm{GW/cm^2}$, the response morphology of the tungsten surface changes, as seen in Fig. 4. Certain degree of plasticity causes that the brittle cracking mechanism changes into a ductile one. Micrographic analysis indicates a strong cavitation in the plastic zone and the cavitation cracking along the grain boundaries (inter-granular cracking).

In contrast to the previous case where the broken bond percolation and coalescence were the basic mechanisms of the crack growth, in this case we have the vacancy generation in the plastic zone, then vacancy percolation and clustering into a cavity. The cavities aggregate on the grain boundaries of various types (the cusp, the triple junction, etc.), and further grow up by the vacancy diffusion until they finally coalesce into a crack.

Triple junction seems to be a basic configuration for the cavity aggregation, and therefore various stages of the crack evolution have the same (Y) configuration.

Typical triangular crack configurations are shown in Fig. 5. For the evolution model of the triangular crack we suggest the model derived from the Miller and Pilkington line-crack model[11].

Fig. 5. Characteristic types of the triangular crack formed at the triple junction as the cavity aggregation center.

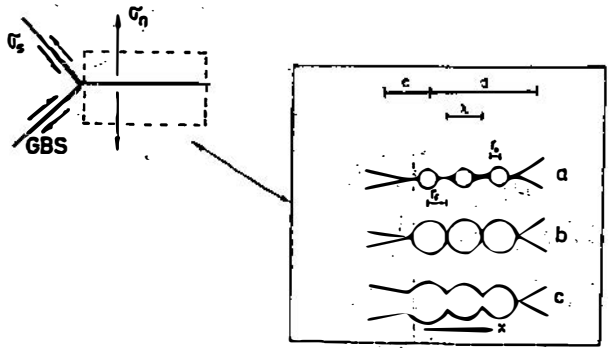

Fig. 6. Schematic illustration of the cavity growth and coalescence on one of the three grown lines of the triple junction (according to Miller and Pilkingotn).

Consider the growth of a crack on a triple junction grain boundary, which is the stress concentration site. Suppose, that the grain boundary cavity structure has been formed ahead of the crack tip, and consider the process on the only one

of the three grain boundary lines. On this line we have a crack of the length c, (Fig. 6a) advancing into a network of cavities.

Suppose that the cavities are of the spherical shape of radius r_0 and spacing λ on a boundary facet of the length d (d = grain size). The cavities will grow by a surface diffusion of vacancies mechanism. Cavities are able to grow until they have a radius equal to $\lambda/2$ (Fig. 6b).

In accordance with Thouless et al.[17], instead of the constant-radius cavities, we shall assume the gradient of cavity sizes along the boundary facet decreasing in size as the distance increases from the crack tip. Now, we can apply this description on the three grain boundary lines of the triple junction. The biggest cavities will be near the center, and the decreasing gradient of sizes will be oriented from the center to the periphery along the grain lines. Therefore, the cracks will advance radially from the center to the periphery of the triple junction site.

In this case we have three big cavities in the junction center, which finally touch each other and coalesce into a bigger one. The high stress concentration and high diffusivity of vacancies cause that the big central cavity appears spherical, i. e. of the equilibrium shape. This model of cavity aggregation, starting from the center and advancing toward the periphery, represents the first phase of the cavity aggregation, which can be seen in Fig. 7.

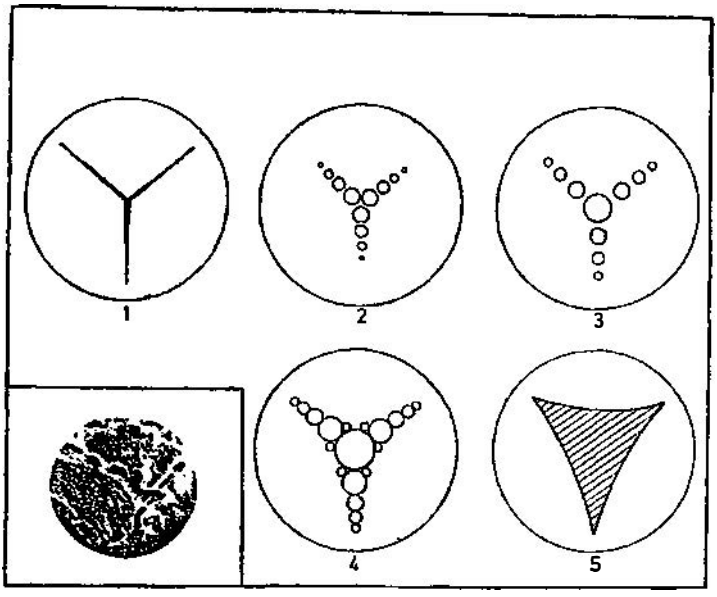

Fig. 7. The five stages of growth of the triangular crack. Primary cavitation phase: 1) triple junction, 2) percolation of cavities on triple junction, 3) cavity coalescence in the center. The second cavitation phase: 4) percolation of the smaller cavities off-the-grain boundary, and their coalescence. 5) Coalescence of the grain boundary and off-the-grain boundary cavities into the triangular crack. (The insert micrography indicates one of the stages of the described process of the triangular crack growth. Formation of the big central cavity in the triple junction is clearly seen).

However, if we assume that the cavity aggregation process occurs only along the grain boundaries, we can get only the crack of the (Y) type, or of the wedge type, and not of the triangular (∇) type.

To get a triangular crack we must allow the cavity aggregation around the triple junction from all directions, which is reasonable at high stresses and temperatures. Thus, in the second phase of the cavity aggregation, the crack will advance by the area-growth, instead of the (grain boundary) line growth.

Therefore, we belleve that the cavitation (by vacancy diffusion) is the grain boundary line process (primary cavitation phase). In the second phase cavitation is off-the-grain boundary line processes. In this secondary phase of cavitation, smaller and smaller cavities aggregate around the (Y) type of skeleton.

Thus, the primary cavitation phase establishes the size of the triangle and the secondary cavitation phase fills up the triangle's area.

3.2.1. *The crack velocity and the crack size*

We shall make a small digression from the topological and geometrical aspect and evaluate the crack velocity and the crack size (size of the triangle) from the fracture mechanics aspect. The crack shape is almost equilateral triangle. Fig. 5. It means that the cavitation process is equal along the 3 given lines of the Y skeleton, and the crack velocity in these directions is equal too. Estimation of the crack velocity and of the crack size (from the center of traingle to the corners), can be done on the basis of the model of Miller and Pillington[16]. For the velocity V_c, one finds[16]:

$$V_c = \frac{1}{2\sqrt{2}} \frac{D_s \Omega^{4/3}}{kT^2 \gamma_s} \frac{1}{(1 - \gamma_{B/2}\gamma_s)^3} \frac{\lambda^3 K^3}{(a\pi)^{3/2}} \frac{1}{(\lambda/2 - r_0)^4} \sqrt{\frac{1}{d}} \left(\frac{d}{\lambda}\right). \tag{4}$$

which gives a K^3 dependence of V_c.

In this equation

D_s = surface diffusion coefficient
k = Boltzmann constant
γ_s = surface energy
γ_B = grain boundary energy
T = temperature (K)
Ω = atomic volume
λ = cavity spacing
r_0 = starting cavity radius
K = stress intensity factor given by linear elasticity

$$\sigma_n = \frac{K}{\sqrt{a\pi x}} \tag{5}$$

σ_n = stress acting normally on the given boundary
x = distance from the crack tip
a = geometric factor.

On this basis we shall try to estimate the crack advancement from the center of the triple junction to the periphery, along one of its 3 directions.

Since the temperature in experiment is $T \approx 0.3\ T_m$ (T_m (W) = 3387 °C), one has $T \approx 1288$ K.

$$\lambda \text{ (experiment)} \approx 4 \cdot 10^{-6} \text{ m}$$

$$d \text{ (experiment)} \approx 20 \cdot 10^{-6} \text{ m}$$

$$r_0 \text{ (experiment)} \approx 3 \cdot 10^{-7} \text{ m}$$

$$\Omega \text{ (W)} = 15.83 \cdot 10^{-30} \text{ m}^3$$

$$k = 1.38 \cdot 10^{-23} \text{ J K}^{-1}$$

$$\gamma_s = 4 \text{ J m}^{-2} \text{ (Ref. 18, Tab. 4)}$$

$$\alpha = 0.248.$$

Two of the tungsten parameters, γ_B, D_s have not been available and for this estimation we have used $\gamma_B \approx 0.78 \text{ J m}^{-2}$ and $D_s \approx 9.4 \times 10^{-15} \text{ m}^2 \text{ s}^{-1}$ relating to the 1 Cr MoV steel Ref. 19. The last missing parameter the stress intensity factor K will be found on the basis of the following procedure:

The laser generated stress σ_L according to Cleur et al.[20] and Yang[21], lies between $10 \cdot 10^8$ Pa and $15 \cdot 10^8$ Pa in this type of experiment. The stress concentrating factor σ_n/σ_L is found to be between 10 and 10^2. [σ_n/σ_L is taken as an equivalent of σ_n/σ_∞ in the tensile stress experiments, which for $T/T_m \approx 0.3$—0.4, and for the stress deposition time of $\approx 18 \cdot 10^{-3}$ s, in a quasicontinuous process, gives 10—10^2. For nickel this can be seen in Ref. 19, and for the other metals in references cited there. The stress deposition time of $18 \cdot 10^{-3}$ s is the time needed to the train of $N = 18$ pulses ($N = vw/\pi v$ at $v = 6$ K Hz, $w = 45 \cdot 10^{-6}$ m, $v = 5 \cdot 10^{-3}$ m/s), to pass over the gives surface point].

Taking the conservative value for the stress concentrating factor $\sigma_n/\sigma_L = 10$, one finds for the locall stress on the given boundary:

$$\sigma_n = 150 \cdot 10^8 \text{ Pa.}$$

Inserting this value into the Eq. (5), and using $x \approx 4 \cdot 10^{-6}$ m, one finds for the stress intensity factor:

$$K \approx 30 \text{ MN m}^{-3/2}. \qquad (6)$$

The crack velocity, V_c, obtained on the basis of the above parameters from the Eq. (4), is:

$$V_c \approx 0.02 \text{ m/s} = 0.2 \text{ μm/ms.}$$

We shall suppose that the crack growth is a quasicontinuous process which occurs in the seedy state conditions. This supposition holds if the cavity incubation time is much shorter than the time to fracture, and if the deformation does not

take place (19). In this case, the crack growth occurs in ≈ 18 ms, which gives for the total length of the crack:

$$l = 0.2\ \mu\text{m/ms} \times 18\ \text{ms} = 3.6\ \mu\text{m}.$$

This value is in a good agreement with the distance from the center of triangle to the corner, for triangular cracks shown in Fig. 5. The lateral size of traingle, L, is $L = 4/\sqrt{3}\ l \approx 8.2\ \mu$m, which also can be compared to the triangles shown in Fig. 5. This is an argument in favour that the size of the traingle is established by the process described in the previous section.

3.2.2. *Iterative filling of space with cavities*

Supposing that the spherical cavities touch each other in one point on their equatorial cross-section, the 3D problem is reduced into a 2-Dimensional one. From the geometrical point of view, one can ask how many circles can be packed together in a triangle. Evidently, the problem is transformed into the Apollonian gasket problem, which again is of the fractal nature[22]. Here we shall refer to the work of De Gennes et al.[23] discussing some features of the iterative filling of space by tangent circles of decreasing size (gradient of sizes). They have treated the statistical properties of focal conic textures in smectic — A liquid crystal, but the problem is general and may include the boundary problems in magnetic materials superfluids and superconductors. It is actually a »domain problem«, which in our case may be understood as a problem of »damaged domains« in metals.

3.2.3. *Apollonian packing of circles*

Let us suppose that the cavities are the spherical hollow balls. In the plane of equatorial cross-sections of the decreasing size hallow balls we have a set of tangent circles (Fig. 8). The three of the neighbour tangent circles in Fig. 8 define a triangle interstice. This empty interstice may be filled up by a foruth circle,

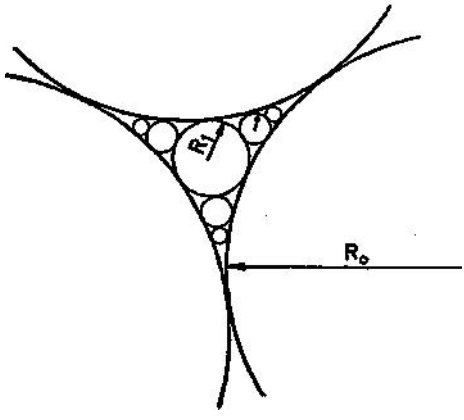

Fig. 8. The iterative filling of triangle in the equatorial plane of the spherical cavities (De Gennes).

tangent to the first three. Thus, a new smaller triangle interstices are generated, which may be filled up by smaller circles, etc. The iteration procedurde starts with the equally large circles (in the first generation of circles). Then, follows the iteration inside one interstice between them[23].

We have payed attention to the packing of cavities and performed measurements of the cavity radius in the series R_m ($m = 1, 2, 3, 4, \ldots$) of successively packed cavities (from the center of triangle to its corner), on the micrographies similar to the one shown in the insert of Fig. 7.

Since the measurements are difficult because of the shadow at the edge of the cavities, and since some of them seems to be slightly elongated spheres, we have given their radii as the interval values, as seen from the Table 1.

TABLE 1.

R_m	Experimental (μm)	Calculated (μm)
R_1	1.15—1.26	1.258
R_2	0.66—0.74	0.731
R_3	0.43—0.55	0.434
R_4	<0.35	0.287

By using the relation[23]

$$R_m \approx \frac{L}{(m + m_0)^2}, \tag{7}$$

where L is the lateral size of triangle ($L \approx 8.20$ μm), m_0 is constant for the partial iteration, or filling up of the triangle with the successive set of circles, we found $m_0 = 1.35$, and calculated the series of the radii R_m ($m = 1$—4). They are also given in Table 1, and show a good agreement with the measured radii up to the R_3. Measurements beyond R_3 are not certain and require a better resolution than we had. The agreement of the measured and calculated radii of the successively packed cavities up to R_3 is very nice and although the R_m series is rather short, it is an argument in favour of packing of the cavities into triangle in the Apollonian way.

The dimension of the largest ball is associated with the size of the triangular crack, L. One can assume further down to circles of radius $\geq \varrho$ ($\varrho \ll L$). The number of circles filling the space at this stage is $g(\varrho)$, which depends only on the ratio ϱ/L[23].

De Gennes has shown that g is of the form[23]:

$$g = Cte \left(\frac{L}{\varrho}\right)^n; \quad (L \gg \varrho) \tag{8}$$

where, n, is the scaling index, which is $1/2 \leq n \leq 2$. Various other calculations which may be found in literature referenced by De Gennes and Mandelbrot [13] give the value of n, between 1.30 and 1.32.

Coming back to our problem of the fractal growth of the triangular crack, we believe that above discussed model could be applied to the catastrophic response patterns seen in Fig. 5.

4. *Conclusion*

Variation of the power density scale from 3.4 GW/cm^2 to 1.4 GW/cm^2, switches the laser-metal interaction into the laser-plasma + laser-metal one. Therefore, the pressure shock induced effects switch to the pressure shock + temperature surface effects. As a consequence, the following changes in the catastrophic response of the surface can be observed.

a) the line-crack morphology changes into the triangular one
b) transgranular cracking changes into integranular one
c) brittle cracking changes into ductile one
d) percolation of the individual broken bonds changes into the percolation of cavities
e) aggregation of the broken bonds into a line crack, changes into the aggregation of cavities into the triangular crack.
f) the fractal family structure and the fractal dimension changes from $D = 1.65$ to $D = 1.32$. (The latter dimension remains to be confirmed in the future measurements).

From the topological and geometrical point of view and on the above basis we suggest that the system reacts on the change of the power density scale, by changing the dimension of the fractal space. Since, the fractal dimension is the space property, the system reacts by changing the properties of the space.

Acknowledgement

The authors are thankful to Dr V. Kraševec from the Jožef Stefan Institute, Ljubljana for the electron microscopy of the laser treated samples, and to Prof. A. Bjeliš from the Faculty for Natural Sciences and Mathematics, University of Zagreb, for the critical reading of the manuscript.

References

1) G. A. Askaryan and M. S. Rabinovich, Zh. Eksp. Teor. Fiz. **48** (1965) 290;
2) Y. P. Raizer, Zh. Eksp. Theor. Fiz. **48** (1965) 1508;
3) S. A. Metz, L. R. Hettche, R. L. Stegman and J. T. Schriemph, J. Appl. Phys. **46** (1975) 1634;
4) A. W. Ehler, J. Appl. Phys. **37** (1966) 4962;
5) R. T. Brown and D. C. Smith, Appl. Phys. Lett. **22** (1973) 245;
6) J. D. O'Keefe, C. H. Skeen and C. M. York, J. Appl. Phys. **44** (1973) 4622;
7a) S. Lugomer, M. Stipančić and M. Kerenović, Vacuum (in press);

7b) S. Lugomer, Vacuum (submitted for publication);
7c) S. Lugomer et al. (in preparation);
8) B. B. Mandelbrot, *The Fractal Geometry of Nature*, Freeman, San Francisco, 1982 (p. 109);
9) C. W. Lung, in *Fractals in Physics*, ed. by L. Pietronero and F. Tossati, North Holland, Amsterdam, 1986, (p. 189);
10) P. Meakin, G. Li, L. Sander, E. Louis and F. Guinea, preprint 1988;
11) E. Louis, F. Guinea and F. Flores, in Ref. 9 (p. 177);
12) E. Louis and F. Guinea, Europhys. Lett. **3** (1987) 871;
13) H. Takayasu, Progr. Theor. Phys. **74** (1985) 1343;
14) H. Takayasu, in ref. 9 (p. 181);
14a) H. J. Hermann and S. Roux, *Statistical Models for the Fracture of Disordered Media*, North Holland, Amsterdam, 1991;
14b) H. J. Hermann (private communication);
15) T. A. Witten and L. M. Sander, Phys. Rev. **B27** (1983) 5686;
16) D. A. Miller and R. Pilkington, Metal. Transact, **11A** (1980) 177;
17) M. D. Thouless, C. H. Hsueh and A. G. Evans, Acta Metall. **31** (1978) 1675;
18) C. Ghandi and M. F. Ashby, Acta Metall. **27** (1979) 1565;
19) M. H. Yoo and H. Trinkans, Metall. Trans. **14A** (1983) 547;
20) A. H. Clauer, B. P. Fairand and B. A. Wilcox, Metall. Trans. **8A** (1977) 119;
21) L. C. Yang, J. Appl. Phys. **45** (1974) 2601;
22) B. B. Mandelbrot, Fractals, Form, Chance and Dimension, W. H. Freeman and Comp. San Francisco, 1977;
23) R. Bidaux, N. Boccarta, G. Sarma, L. de Seze, P. G. De Gennes and O. Parodi, J. de Physique **34** (1973) 661.

LASERSKI-INDUCIRANO FRAKTALNO PUCANJE POVRŠINE TUNGSTENA

STJEPAN LUGOMER

Institut »Ruđer Bošković«, P. O. B. 1016, 41001 Zagreb

MLADEN STIPANČIĆ

Elektrotehnički fakultet, Univerzitet u Banja Luci, 78000 Banja Luka

UDK 538.951

Originalni znanstveni rad

Katastrofični odziv površine tungstena u laser-materijal interakciji, izazvanoj Q-switched Nd:YAG laserom, na srednjoj gustoći snage $\overline{Q} = 1.4$ GW/cm^2—3.5 GW/cm^2, pojavljuje se u dvije morfologije pucanja: kao linearno lomno (brittle) pucanje i kao duktilno trokutasto pucanje. Oba tipa pukotina mogu se tretirati kao fraktalni objekti. Za prvi tip pukotina nađena je fraktalna dimenzija $D = 1.60$ i dana je komparacija s modelom Louisa i suradnika, za mehanički slom elastičnih materijala, kao i sa deterministčkim modelom Takayasu-a. Za drugi tip pucanja sugeriran je kavitacijski mehanizam nastajanja na granicama trostrukog spoja metalnih zrna. Njegovo fraktalno modeliranje bazirano je na »Apollonian gasket« modelu, koji daje dimenziju $D = 1.32$.